# Using Pyridinyl-Substituted Diaminotriazines to Bind Pd(II) and Create Metallotectons for Engineering Hydrogen-Bonded Crystals

Adam Duong, Thierry Maris, and James D. Wuest*

Département de Chimie, Université de Montréal, Montréal, Québec H3C 3J7, Canada

S *Supporting Information*

ABSTRACT: The pyridinyl groups of pyridinyl-substituted diaminotriazines **3a,b** and **4a,b** can bind metals, and the diaminotriazinyl (DAT) groups serve independently to ensure that the resulting complexes can participate in intercomplex hydrogen bonding according to characteristic motifs. As planned, ligands **3a,b** and **4a,b** form trans square-planar 2:1 complexes with $PdCl_2$, and further association of the complexes is directed in part by hydrogen bonding of the DAT groups. Similarly, ligands **3a,b** and **4a,b** form cationic square-planar 4:1 complexes with $Pd(BF_4)_2$, $Pd(PF_6)_2$, and $Pd(NO_3)_2$, and the complexes again typically associate by hydrogen bonding of the peripheral DAT groups. The observed complexes have predictable constitutions and shared structural features that result logically from their characteristic topologies and the ability of DAT groups to engage in hydrogen bonding. These results illustrate the potential of a hybrid inorganic/organic strategy for constructing materials in which coordinative bonds to metals are used in conjunction with other interactions, both to build the molecular components and to control their organization.
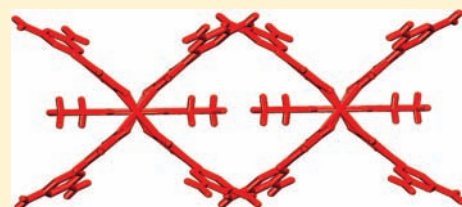
INTRODUCTION

For nearly a century, X-ray diffraction has been used to reveal the atomic structure of crystals.[1] During that time, more than 500 000 structures of molecular crystals have been resolved and catalogued.[2] Despite the imposing mass of collected data, however, full understanding of the factors underlying structural preferences remains elusive.[3] Each added structure is unique, and its crystallographic parameters cannot be predicted reliably. Designing new molecular crystals and other ordered materials is a profoundly difficult enterprise, yet it is essential for progress in many areas of science and technology. Under these circumstances, qualitative guidelines for controlling molecular organization are indispensable and must be improved.

A widely used approach is based on the concept of building ordered materials by the spontaneous association of tectons, which are molecules with suitable topologies and an ability to engage in multiple predictable interactions with neighbors.[4] When properly exploited, this approach can yield materials with predetermined organization and with collective properties that depend on those of the individual molecular components, modified in a programmable way by the effect of their neighbors. Even though structural parameters cannot be predicted reliably in detail, this strategy allows gross features to be introduced with confidence, and it will continue to be an important source of new molecular materials.

This strategy must be further tested and refined by using it to build materials from the widest possible range of molecular components, held together by a full spectrum of interactions that meet basic criteria of strength and reliability. Most tectons that have been studied so far are typified by structure **1**, which

consists of a covalently bonded molecular core, functionalized by multiple peripheral groups (●) that engage in interactions according to established patterns. Covalently bonded cores are attractive because they are robust, but they must often be made laboriously by multistep syntheses. An appealing alternative is the self-assembly of topologically related tetrahedral or square-planar structures represented by metallotecton **2**, which is held together by coordinative bonds to a metal.[5−7] Moreover, this alternative approach allows the geometry of coordination to be altered systematically by varying the metal. Despite the conspicuous advantages of this strategy, metallotectons remain underexploited in the effort to engineer new materials, possibly because their use requires a dual understanding of both organic and inorganic chemistry.
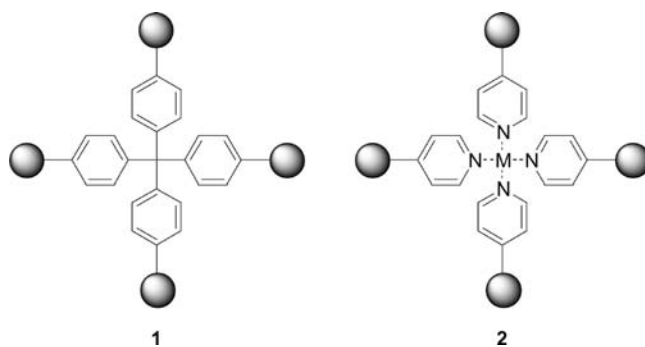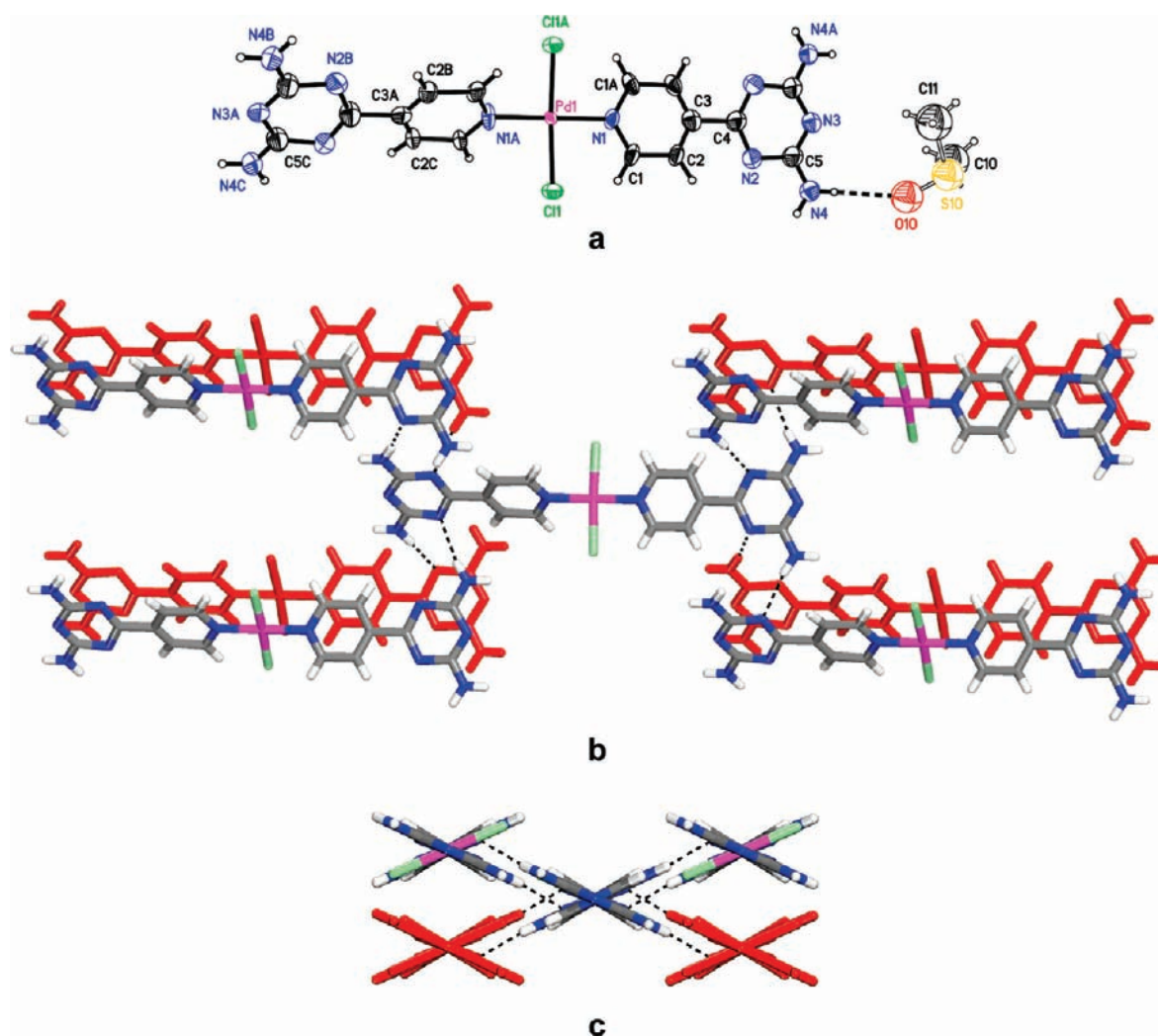
Figure 1. Structure of complex PdCl$_2$(**3a**)$_2$·2DMSO in crystals grown from DMSO/H$_2$O. Hydrogen bonds are represented by broken lines. Except where noted otherwise, carbon atoms are shown in gray, hydrogen atoms in white, nitrogen atoms in blue, oxygen atoms in red, sulfur atoms in yellow, chlorine atoms in green, and palladium atoms in rose. (a) Thermal atomic displacement ellipsoid plot, with ellipsoids of non-hydrogen atoms drawn at the 50% probability level and hydrogen atoms represented by a sphere of arbitrary size. Key bond lengths include Pd1—N1 = 2.012(18) Å and Pd1—Cl1 = 2.309(3) Å. Key bond angles include Cl1—Pd1—Cl1A = 177.0(6)°, N1—Pd1—N1A = 180°, and N1—Pd1—Cl1 = 91.5(3)°. (b) View along the *a* axis showing eight N—H···N hydrogen bonds of modified type **III** (3.103(12) Å) formed by the central metallotecton and eight neighbors, four in an upper plane (normal colors) and four in a lower plane (red). Guest molecules of DMSO are omitted for clarity. (c) Alternative view along the *c* axis showing the relationship between the central metallotecton and its neighbors.

To further explore the potential of this approach, we elected to study the behavior of metallic complexes of substituted pyridine **3a**[8] and its elongated derivative **3b**,[9] as well as their isomers **4a**[10] and **4b**.[11] The design of this set of ligands is based on the well-established ability of pyridines to bind metals, combined with the tendency of diaminotriazinyl (DAT) groups to engage in multiple hydrogen bonds according to motifs **I**—**III**.[12] Pyridines are typically stronger ligands than triazines, so we expected the two distinct parts of compounds **3a,b** and **4a,b** to operate orthogonally, one to ensure formation of a metallotecton by coordination and the other to direct intermolecular association by hydrogen bonding. In initial work, we decided to examine the ability of ligands **3a,b** and **4a,b** to bind Pd(II), which is known to favor related complexes with a square-planar geometry.[13,14] By focusing on a single metal with a predictable geometry of coordination, bound by a family of ligands that vary systematically, we designed our study to produce a set of closely related structures

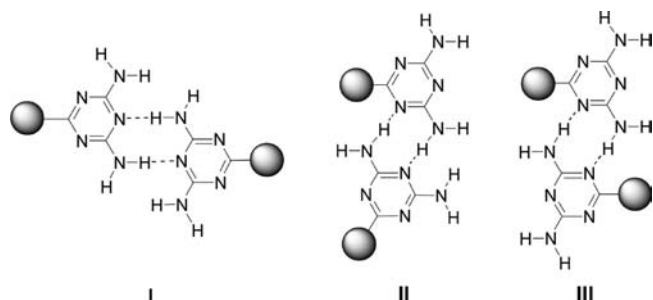that can be compared to reveal basic principles of metallotectonic assembly.
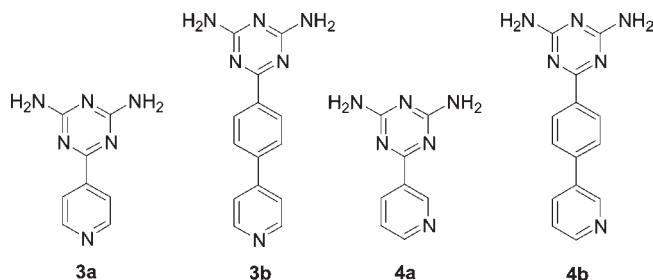
RESULTS AND DISCUSSION

Syntheses of Ligands 3a,b and 4a,b. 6-(Pyridin-4-yl)-1,3, 5-triazine-2,4-diamine (**3a**),[8] 6-[4-(pyridin-4-yl)phenyl]-1,3,

Table 1. Crystallographic Data for 1:2 and 1:1 Complexes of PdCl$_2$ with Pyridinyl-Substituted Diaminotriazines 3a,b, 4a,b, and 6

| complex	PdCl$_2$(3a)$_2$·2DMSO	PdCl$_2$(3a)$_2$·2DMSO·dioxane	PdCl$_2$(3b)$_2$	PdCl$_2$(4a)$_2$·3DMSO	PdCl$_2$(6)
crystallization medium	DMSO/H$_2$O	DMSO/dioxane	DMSO/EtOAc	DMSO	DMSO/H$_2$O
formula	C$_{20}$H$_{28}$Cl$_2$N$_{12}$O$_2$PdS$_2$	C$_{24}$H$_{36}$Cl$_2$N$_{12}$O$_4$PdS$_2$	C$_{28}$H$_{24}$Cl$_2$N$_{12}$Pd	C$_{22}$H$_{34}$Cl$_2$N$_{12}$O$_3$PdS$_3$	C$_8$H$_8$Cl$_2$N$_5$Pd
cryst syst	orthorhombic	triclinic	monoclinic	monoclinic	monoclinic
space group	$I222$	$P\bar{1}$	$P2_1/n$	$C2/c$	$P2_1/n$
a (Å)	3.7721(10)	6.1250(8)	13.6163(10)	37.2003(9)	7.9908(3)
b (Å)	11.346(3)	9.7568(13)	10.9178(9)	8.0105(2)	9.1500(4)
c (Å)	28.990(7)	15.6448(18)	18.8566(15)	11.0946(3)	15.4450(16)
α (deg)	90	105.458(6)	90	90	90
β (deg)	90	96.393(6)	93.775(3)	93.530(1)	98.586(2)
γ (deg)	90	97.755(7)	90	90	90
V (Å^3)	1240.7(6)	882.19(19)	2797.1(4)	3299.84(15)	1116.62(8)
Z	2	1	4	4	4
ρ_{calc} (g cm^{-3})	1.900	1.502	1.676	1.586	2.174
T (K)	100	150	150	100	150
μ (mm^{-1})	10.014	7.152	7.477	8.192	17.711
R_1, $I > 2\sigma(I)$	0.0734	0.0491	0.0583	0.0235	0.0263
R_1, all data	0.0740	0.0533	0.0623	0.0248	0.0290
wR_2, $I > 2\sigma(I)$	0.1754	0.1340	0.1350	0.0659	0.0709
wR_2, all data	0.1758	0.1377	0.1355	0.0669	0.0721
measured reflns	2699	12588	30310	25455	14799
independent reflns	1091	3156	5280	2910	2213
observed reflns [$I > 2\sigma(I)$]	1023	2882	3201	2761	2027

I   **II**   **III**

5-triazine-2,4-diamine (**3b**),[9] 6-(pyridin-3-yl)-1,3,5-triazine-2,4-diamine (**4a**),[10] and 6-[4-(pyridin-3-yl)phenyl]-1,3,5-triazine-2,4-diamine (**4b**)[11] were prepared by reported methods.

Structures of Unbound Ligands 3a,b and 4a,b. To provide a basis for understanding the association of metallotectons derived from compounds **3a,b** and **4a,b**, we examined the structures of crystals of the unbound ligands themselves in a preliminary study.[11] A comparison of the structures identified three shared features: (1) The compounds adopt flattened conformations typical of aryl-substituted triazines;[12] (2) they form approximately coplanar hydrogen bonds according to characteristic motifs **I**–**III**; and (3) these interactions play a major role in directing molecular organization. Because compounds **3a,b** and **4a,b** have similar flattened molecular shapes and incorporate DAT groups, they crystallize similarly to give hydrogen-bonded structures built from chains, tapes, and layers. The same factors can be expected to help direct the association of metallotectons derived from compounds **3a,b** and **4a,b** when they are used as ligands.

Syntheses and Structures of Complexes of Ligands 3a,b and 4a,b with PdCl$_2$. Complexes were prepared by mixing the ligands (2 equiv) with PdCl$_2$ (1 equiv) in MeCN. The precipitated solids were then crystallized, and the structures were determined by X-ray crystallography.

*a. Structures of the 2:1 Complex of 6-(Pyridin-4-yl)-1,3,5-triazine-2,4-diamine (**3a**) with PdCl$_2$.* Pyridine itself is known to react with PdCl$_2$ to give square-planar complex **5** with trans-oriented pyridinyl ligands,[13] so we expected ligand **3a** to yield an analogous 2:1 complex.

5   **6**   **7**
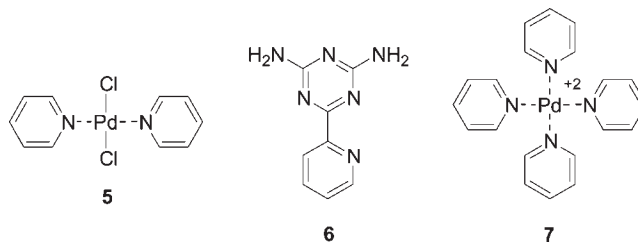
Crystals grown from DMSO/H$_2$O were found to have the composition PdCl$_2$(**3a**)$_2$·2DMSO and to belong to the orthorhombic space group $I222$. Views of the structure are provided in Figure 1, and other crystallographic data are presented in Table 1. As anticipated, the pyridinyl groups of compound **3a** are bound in a trans orientation to give a square-planar Pd(II) complex (Figure 1a), with normal Pd—N and Pd—Cl distances.[13] The pyridinyl and triazinyl rings in each ligand are nearly coplanar, as expected,[12] and the torsional angle between the average planes is only 4.8(6)°. The average planes of the two trans-oriented ligands form an angle of 50.6(2)° with respect to each other, and they lie at angles of 1.3(3)° and 49.4(1)° with respect to the essentially planar PdN$_2$Cl$_2$ core of the metallotecton.

The resulting metallotecton predictably defines a linear structure with DAT groups at its two extremities. Each DAT group participates in four N—H···N hydrogen bonds according to a modified version of motif **III**, and each metallotecton thereby forms a total of eight hydrogen bonds with eight neighbors to give a three-dimensional network (Figures 1b,c). Channels aligned with
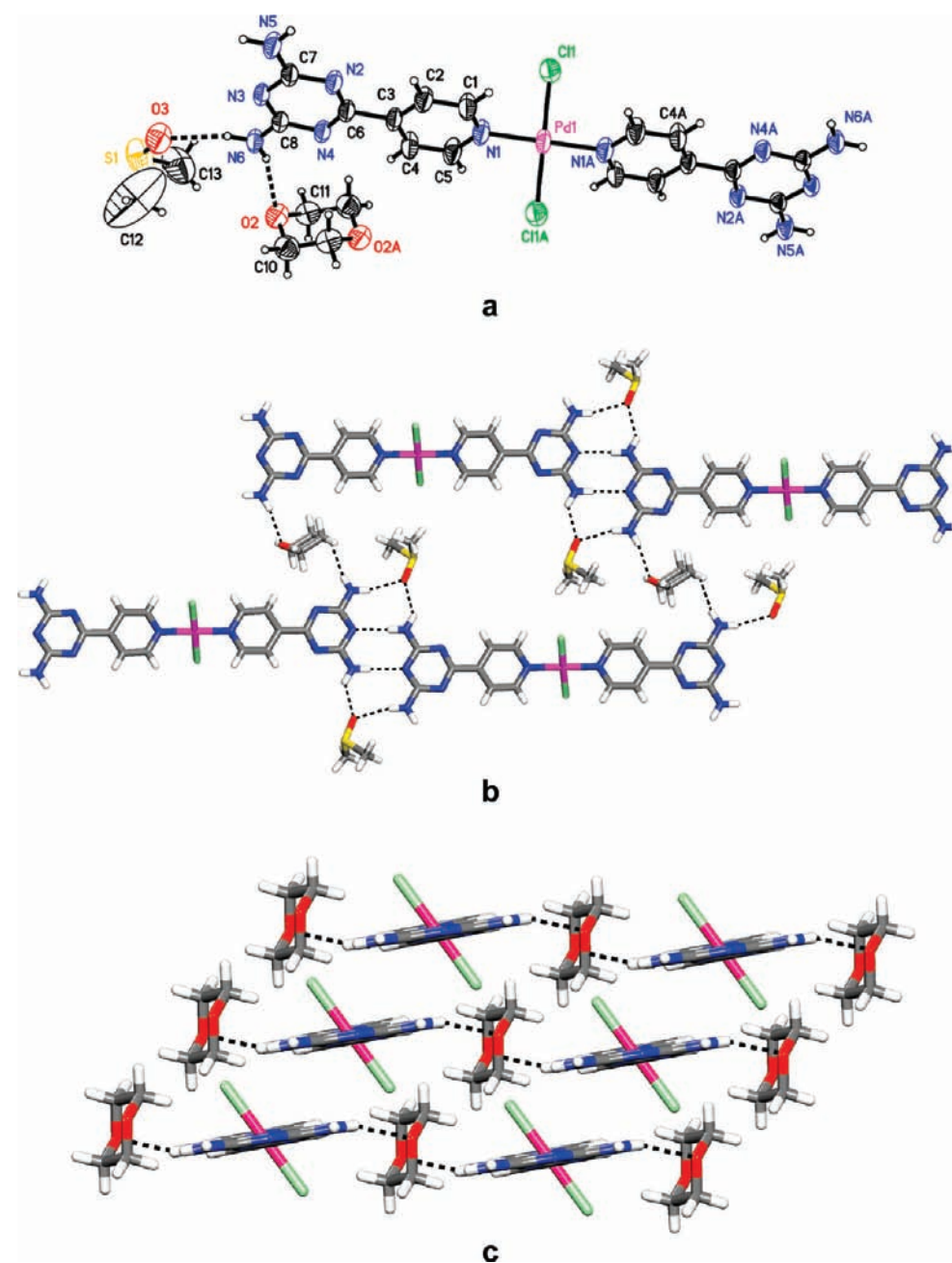
Figure 2. Structure of complex $PdCl_2(3a)_2 \cdot 2DMSO \cdot dioxane$ in crystals grown from DMSO/dioxane. Hydrogen bonds are represented by broken lines. Carbon atoms are shown in gray, hydrogen atoms in white, nitrogen atoms in blue, oxygen atoms in red, sulfur atoms in yellow, chlorine atoms in green, and palladium atoms in rose. (a) Thermal atomic displacement ellipsoid plot, with ellipsoids of non-hydrogen atoms drawn at the 50% probability level and hydrogen atoms represented by a sphere of arbitrary size. Key bond lengths include Pd1—N1 = 2.018(3) Å and Pd1—Cl1 = 2.3207(13) Å. Representative bond angles include Cl1—Pd1—Cl1A = 180°, N1—Pd1—N1A = 180°, and N1—Pd1—Cl1 = 90.20(12)°. (b) View showing how N—H···N hydrogen bonds of type **I** (2.980(5) Å), reinforced by N—H···O hydrogen bonds involving bridging molecules of DMSO (average distance = 2.959(5) Å), link the metallotectons into chains, which are further connected into sheets by N—H···O hydrogen bonds (3.049(5) Å) involving intervening molecules of dioxane. (c) View showing alternating layers of metallotectons and guests, with molecules of DMSO omitted for clarity.

the *a* axis contain disordered molecules of DMSO, which form hydrogen bonds with the DAT groups (Figure 1a) and thereby prevent the metallotectons from associating end-to-end by forming hydrogen bonds of type **I**. As planned, the observed structure is organized by a combination of coordinative interactions and hydrogen bonds. Key features of the structure are a logical result of (1) the tendency of $PdCl_2$ to form trans square-planar

1:2 complexes with pyridines and (2) the creation of a metallotecton with DAT groups at the ends of an elongated linear structure, which favors a parallel alignment held together by hydrogen bonds.

To probe the effect of solvent on the formation and association of metallotectons derived from $PdCl_2$ and ligand **3a**, we also grew crystals from DMSO/dioxane. They proved to have the composition
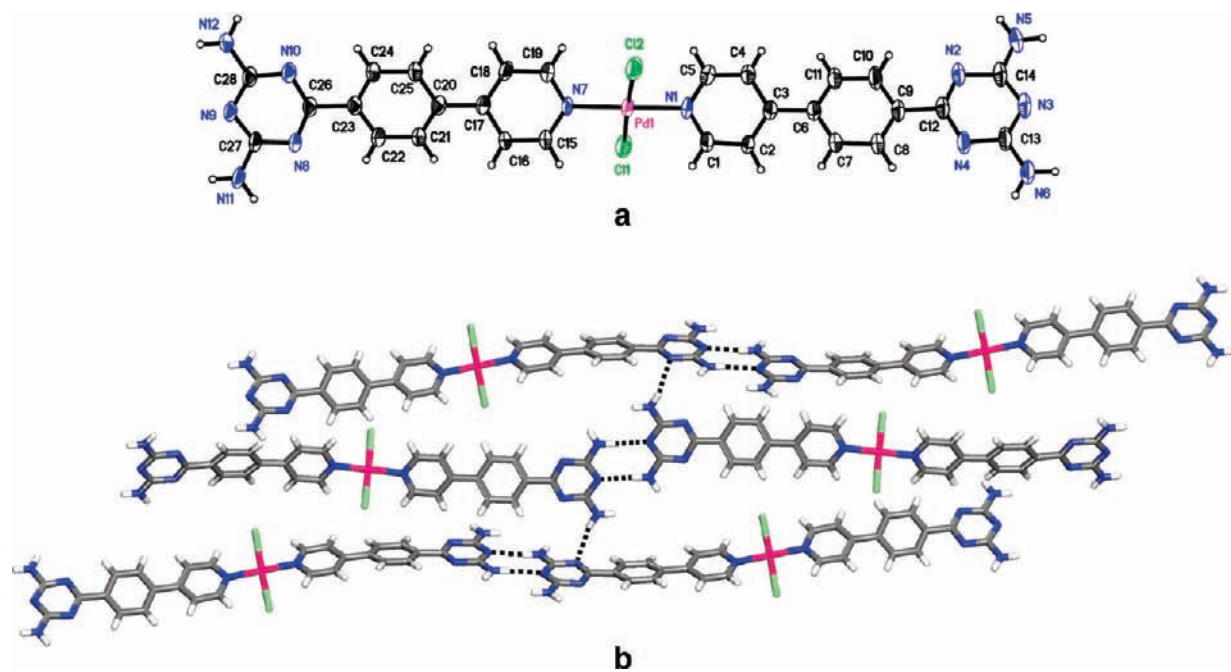
Figure 3. Structure of complex PdCl$_2$(**3b**)$_2$ in crystals grown from DMSO/EtOAc. Hydrogen bonds are represented by broken lines. Carbon atoms are shown in gray, hydrogen atoms in white, nitrogen atoms in blue, chlorine atoms in green, and palladium atoms in rose. (a) Thermal atomic displacement ellipsoid plot, with ellipsoids of non-hydrogen atoms drawn at the 50% probability level and hydrogen atoms represented by a sphere of arbitrary size. Key bond lengths include Pd1−N1 = 2.026(4) Å, Pd1−N7 = 2.033(4) Å, Pd1−Cl1 = 2.3079(15) Å, and Pd1−Cl2 = 2.2968(15) Å. Representative bond angles include Cl1−Pd1−Cl2 = 177.21(5)°, N1−Pd1−N7 = 179.4(2)°, and N1−Pd1−Cl1 = 88.33(15)°. (b) View showing how N−H···N hydrogen bonds of type **I** (2.961(6) Å) link the metallotectons into chains, which are further connected into sheets by edge-to-face N−H···N hydrogen bonds (3.081(6) Å).

PdCl$_2$(**3a**)$_2$·2DMSO·dioxane and to belong to the triclinic space group $P\bar{1}$. Views of the structure are shown in Figure 2, and other crystallographic data are summarized in Table 1. Again, a square-planar complex with trans-oriented pyridinyl groups is formed (Figure 2a), with normal Pd−N and Pd−Cl distances.[13] The pyridinyl and triazinyl rings in each ligand are essentially coplanar, and both ligands lie in the same plane, which forms an angle of 62.7(1)° with the PdN$_2$Cl$_2$ core of the metallotecton.

As shown in Figure 2b, the metallotectons are linked into chains by hydrogen bonding of DAT groups according to motif **I**, reinforced by N−H···O hydrogen bonds involving bridging molecules of DMSO. The chains are further joined to form sheets by N−H···O hydrogen bonds with connecting molecules of dioxane (Figure 2b), and the sheets stack to give a structure that consists of layers of metallotectons separated by intervening layers of DMSO and dioxane (Figure 2c). Together, these results confirm that the product of the reaction of PdCl$_2$ with ligand **3a** can be crystallized under different conditions to give structures built predictably from a metallotecton with a single well-defined constitution. However, the conformation of the metallotecton can vary, thereby allowing somewhat different structures to be formed. Nevertheless, both observed structures predictably share two key features: (1) The elongated linear metallotectons are arranged in a parallel orientation, and (2) they are positioned by multiple coplanar hydrogen bonds involving DAT groups.

*b. Structure of the 2:1 Complex of 6-[4-(Pyridin-4-yl)phenyl]-1,3,5-triazine-2,4-diamine (**3b**) with PdCl$_2$.* On the basis of the observed behavior of 6-(pyridin-4-yl)-1,3,5-triazine-2,4-diamine (**3a**), we expected elongated analogue **3b** to behave in a similar way. Crystals of the complex of PdCl$_2$ with ligand **3b** were grown from DMSO/EtOAc. They were found to have the composition

PdCl$_2$(**3b**)$_2$ and to belong to the monoclinic space group $P2_1/n$. Figure 3 provides views of the structure, and Table 1 contains other crystallographic data. As planned, a square-planar complex with trans-oriented pyridinyl groups is produced (Figure 3a), with normal Pd−N and Pd−Cl distances.[13] The bound ligands adopt nearly planar conformations, and their average planes form similar angles (44.4(1)° and 71.6(1)°) with the PdN$_2$Cl$_2$ core of the metallotecton.

As shown in Figure 3b, the metallotectons are joined to form chains through N−H···N hydrogen bonds of type **I** involving DAT groups, and the chains are further connected to form sheets through edge-to-face N−H···N hydrogen bonds. Again, PdCl$_2$ reacts predictably with ligand **3b** to form a metallotecton that crystallizes to generate a structure with expected features, dictated in part by hydrogen bonding of the DAT groups and by the elongated topology of the molecular constituents, which favors a parallel arrangement.

*c. Structure of the 2:1 Complex of 6-(Pyridin-3-yl)-1,3,5-triazine-2,4-diamine (**4a**) with PdCl$_2$.* To probe the effect of distorting the linear geometry of metallotectons derived from ligand **3a** and its extended analogue **3b**, we grew crystals of the complex of PdCl$_2$ with ligand **4a** from DMSO. They proved to have the composition PdCl$_2$(**4a**)$_2$·3DMSO and to belong to the monoclinic space group $C2/c$. Views of the structure are shown in Figure 4, and other crystallographic data are presented in Table 1. As expected, complexation yields a square-planar complex with trans-oriented pyridinyl groups (Figure 4a), and the Pd−N and Pd−Cl distances are normal.[13] Each bound ligand adopts a flattened conformation, and the two ligands lie in essentially the same plane, which forms an angle of 66.8(1)° with the PdN$_2$Cl$_2$ core of the metallotecton. The two DAT groups are oriented on opposite sides of the PdN$_2$Cl$_2$ core.
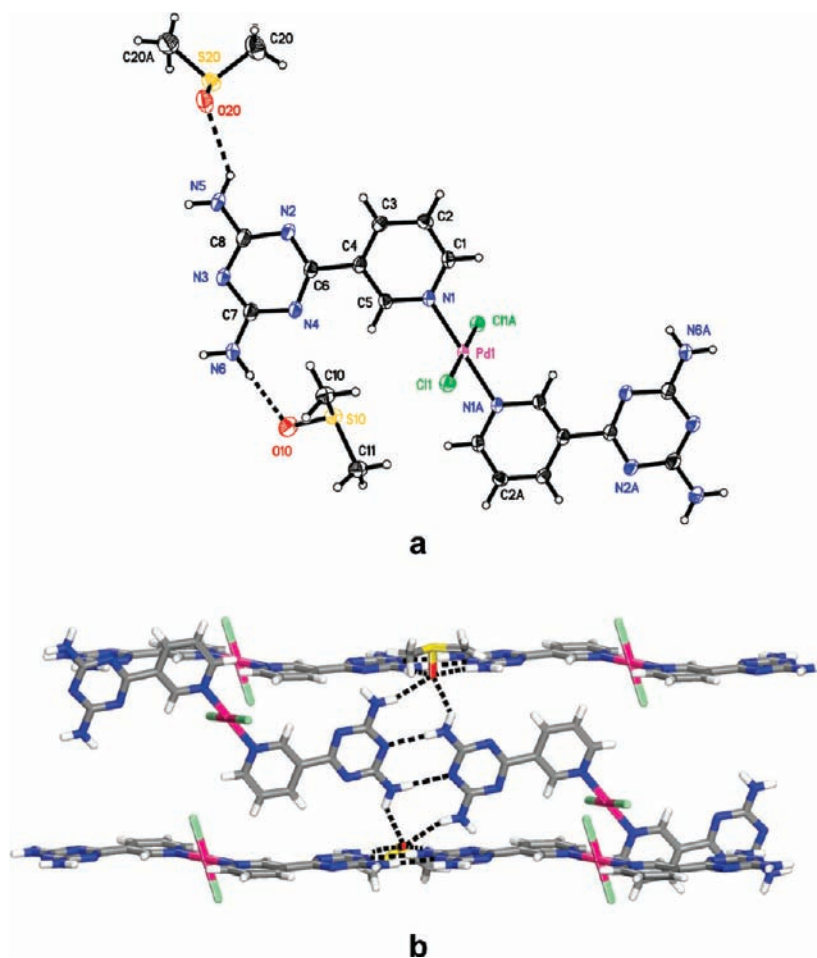
Figure 4. Structure of complex PdCl$_2$(**4a**)$_2$·3DMSO in crystals grown from DMSO. Hydrogen bonds are represented by broken lines. Carbon atoms are shown in gray, hydrogen atoms in white, nitrogen atoms in blue, oxygen atoms in red, sulfur atoms in yellow, chlorine atoms in green, and palladium atoms in rose. (a) Thermal atomic displacement ellipsoid plot, with ellipsoids of non-hydrogen atoms drawn at the 50% probability level and hydrogen atoms represented by a sphere of arbitrary size. Key bond lengths include Pd1−N1 = 2.0150(16) Å and Pd1−Cl1 = 2.2981(5) Å. Representative bond angles include Cl1−Pd1−Cl1A = 180°, N1−Pd1−N1A = 180°, and N1−Pd1−Cl1 = 90.97(5)°. (b) View showing how N−H···N hydrogen bonds of type **I** (2.961(3) Å) link the metallotectons into chains, which interact with adjacent chains by N−H···O hydrogen bonds involving bridging molecules of DMSO.

Although the DAT groups of each metallotecton no longer have a collinear orientation, as maintained in analogous complexes of ligands **3a** and **3b**, association occurs in essentially the same way. Specifically, N−H···N hydrogen bonding of type **I** leads to the formation of zigzag chains, which engage in additional intra- and interchain N−H···O hydrogen bonds involving bridging molecules of DMSO (Figure 4b). Again, complexation of PdCl$_2$ produces a metallotecton with a predictable constitution; furthermore, its elongated geometry and the incorporated DAT groups ensure the formation of a structure in which the components have an approximately parallel orientation and engage in multiple intermolecular hydrogen bonds according to reliable patterns.

Synthesis and Structure of the 1:1 Complex of 6-(Pyridin-2-yl)-1,3,5-triazine-2,4-diamine (6) with PdCl$_2$. Ligands **3a**, **3b**, and **4a** all behave as expected by producing square-planar trans 2:1 complexes with PdCl$_2$ analogous to structure **5**. In these complexes, the pyridinyl and DAT groups operate orthogonally to ensure coordination and intermolecular hydrogen bonding, respectively, without mutual interference. In contrast, ligand **6** promises to allow the two groups to cooperate by chelating

Pd(II). To test this possibility, ligand **6** and PdCl$_2$ were mixed in a 1:1 ratio in MeCN. The precipitated solid was then crystallized from DMSO/H$_2$O, and the structure was determined by X-ray crystallography.

The crystals were found to have the composition PdCl$_2$(**6**) and to belong to the monoclinic space group $P2_1/n$. Views of the structure are presented in Figure 5, and other crystallographic data are provided in Table 1. As expected, complexation yields a square-planar chelate (Figure 5a) with normal Pd−N and Pd−Cl distances.[13] The Pd−N$_{triazine}$ bond is longer than the Pd−N$_{pyridine}$ bond, reflecting the weaker coordination of triazines. The bound ligand is essentially planar and lies close to the average plane of the PdN$_2$Cl$_2$ core of the complex.

The chelates are paired by N−H···N hydrogen bonds of type **I** to form dimers, which associate with adjacent dimers in various ways, such as by forming N−H···Cl interactions (Figure 5b). The structure of the complex is noteworthy because it establishes that compound **6** can serve as a bidentate ligand analogous to 2,2′-bipyridine. This suggests a potentially general strategy in which heteroaromatic groups in other well-known multidentate ligands are replaced with DAT groups to create
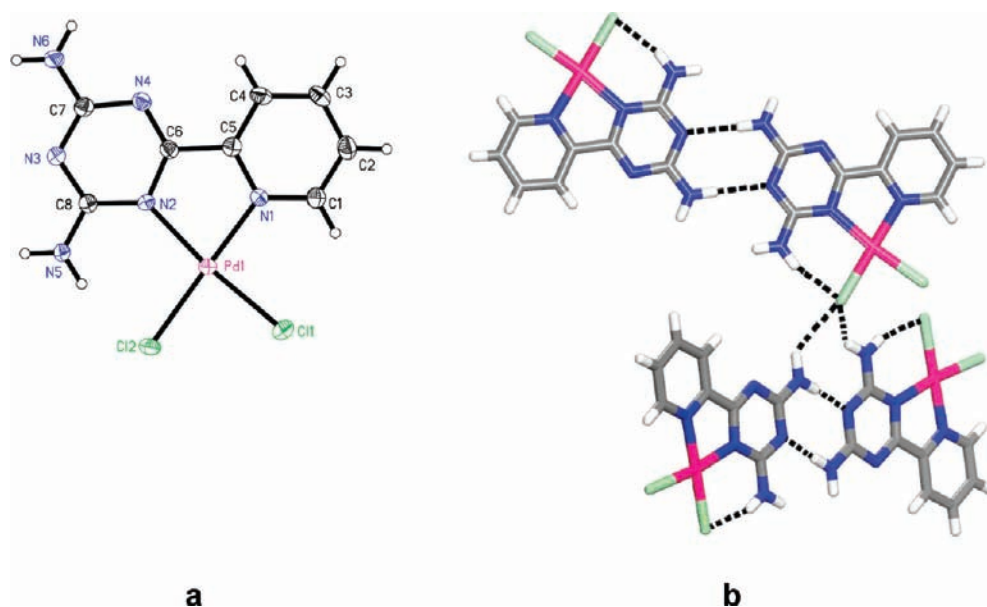
Figure 5. Structure of complex $PdCl_2(6)$ in crystals grown from DMSO/H_2O. Hydrogen bonds are represented by broken lines. Carbon atoms are shown in gray, hydrogen atoms in white, nitrogen atoms in blue, chlorine atoms in green, and palladium atoms in rose. (a) Thermal atomic displacement ellipsoid plot, with ellipsoids of non-hydrogen atoms drawn at the 50% probability level and hydrogen atoms represented by a sphere of arbitrary size. Key bond lengths include Pd1$-$N1 = 2.029(2) Å, Pd1$-$N2 = 2.087(2) Å, Pd1$-$Cl1 = 2.2897(8) Å, and Pd1$-$Cl2 = 2.3041(7) Å. Representative bond angles include Cl1$-$Pd1$-$Cl2 = 86.12(3)°, N1$-$Pd1$-$N2 = 80.54(10)°, N1$-$Pd1$-$Cl1 = 93.06(8)°, and N2$-$Pd1$-$Cl2 = 173.35(7)°. (b) View showing how N$-$H$\cdots$N hydrogen bonds of type **I** (3.023(4) Å) link the chelates into dimers, which associate with adjacent dimers in various ways, such as by forming N$-$H$\cdots$Cl interactions.

surrogates with two characteristic properties: (1) They can chelate metals in analogous ways, and (2) the resulting complexes have similar topologies, but they are endowed with the additional ability to engage in extensive hydrogen bonding according to reliable patterns. However, metallotectons derived from $PdCl_2$ and bidentate ligand **6** have only one DAT group per complex, so they are less able to engage in intermolecular hydrogen bonding than complexes derived from monodentate ligands **3a,b** and **4a,b**, which have two DAT groups. For this reason, we elected to reserve further study of ligand **6** and bidentate analogues for future work and to focus in the present study on the behavior of monodentate ligands **3a,b** and **4a,b**.

Syntheses and Structures of 4:1 Complexes of Ligands 3a, b and 4a,b with $Pd(BF_4)_2$, $Pd(PF_6)_2$, and $Pd(NO_3)_2$. Complexes were prepared by mixing the ligands (4 equiv) with salts of Pd(II) (1 equiv) in MeCN. The precipitated solids were then crystallized, after exchange of anions if needed, and the structures were determined by X-ray crystallography.

*a. Structure of the 4:1 Complex of 6-(Pyridin-4-yl)-1,3, 5-triazine-2,4-diamine (**3a**) with $Pd(BF_4)_2$.* Pyridine reacts with $Pd(BF_4)_2$ to give square-planar dication **7**,[14] so we expected ligand **3a** to yield an analogous 4:1 complex. Crystals grown from DMSO/H_2O/MeCN proved to have the composition $[Pd(3a)_4]$-$(BF_4)_2 \cdot 9H_2O$ and to belong to the monoclinic space group $P2_1/n$. Figure 6 shows views of the structure, and Table 2 summarizes other crystallographic data. As anticipated, the pyridinyl groups of ligand **3a** bind Pd(II) to give a square-planar complex (Figure 6a), with normal Pd$-$N distances.[14] The pyridinyl and triazinyl rings in each ligand are nearly coplanar, and the pyridinyl groups lie essentially perpendicular to the PdN_4 core of the metallotecton, as observed in related structures.[14]

The resulting metallotecton has a molecular structure that adheres closely to expectations; moreover, it appears to be properly

designed to create a robust open rectangular grid held together by hydrogen bonding of four tetragonally directed DAT groups. In fact, however, the observed structure is relatively compact and can be considered to be built from the tetrameric units shown in Figure 6b, in which face-to-face and edge-to-face aromatic interactions of DAT groups are present but normal hydrogen bonds are absent. Interpenetration of the resulting cationic grids (Figure 6c) leads to a three-dimensional structure in which each molecule in a grid forms a total of six N$-$H$\cdots$N hydrogen bonds with six adjacent molecules in an interpenetrating grid (Figure 6d). In addition, H_2O and BF_4^- included within the structure engage in extensive hydrogen bonding.

*b. Structure of the 4:1 Complex of 6-[4-(Pyridin-4-yl)phenyl]-1,3,5-triazine-2,4-diamine (**3b**) with $Pd(NO_3)_2$.* To further assess the potential of pyridinyl-substituted diaminotriazines to form metallotectons related to complex **7**, we examined the product of the reaction of extended ligand **3b** with $Pd(NO_3)_2$. Crystals grown from DMSO/H_2O/MeOH were found to have the composition $[Pd(3b)_4](NO_3)_2 \cdot 5DMSO \cdot 2H_2O \cdot MeOH$ and to belong to the triclinic space group $P\bar{1}$. Views of the structure are presented in Figure 7, and other crystallographic data are provided in Table 2. Again, the pyridinyl groups of the ligand bind Pd(II) to give a square-planar complex (Figure 7a), with normal Pd$-$N distances.[14] The ligands adopt a variety of nonplanar conformations, and their average planes lie at an average angle of 36.0(3)° with respect to the PdN_4 core of the metallotecton.

Two arms of each metallotecton participate in the formation of a total of four N$-$H$\cdots$N hydrogen bonds of type **II** to form characteristic dimers (Figure 7b), which associate with adjacent dimers to form sheets held together by additional N$-$H$\cdots$N hydrogen bonds of type **I**, N$-$H$\cdots$O hydrogen bonds involving bridging molecules of DMSO, and aromatic interactions. All
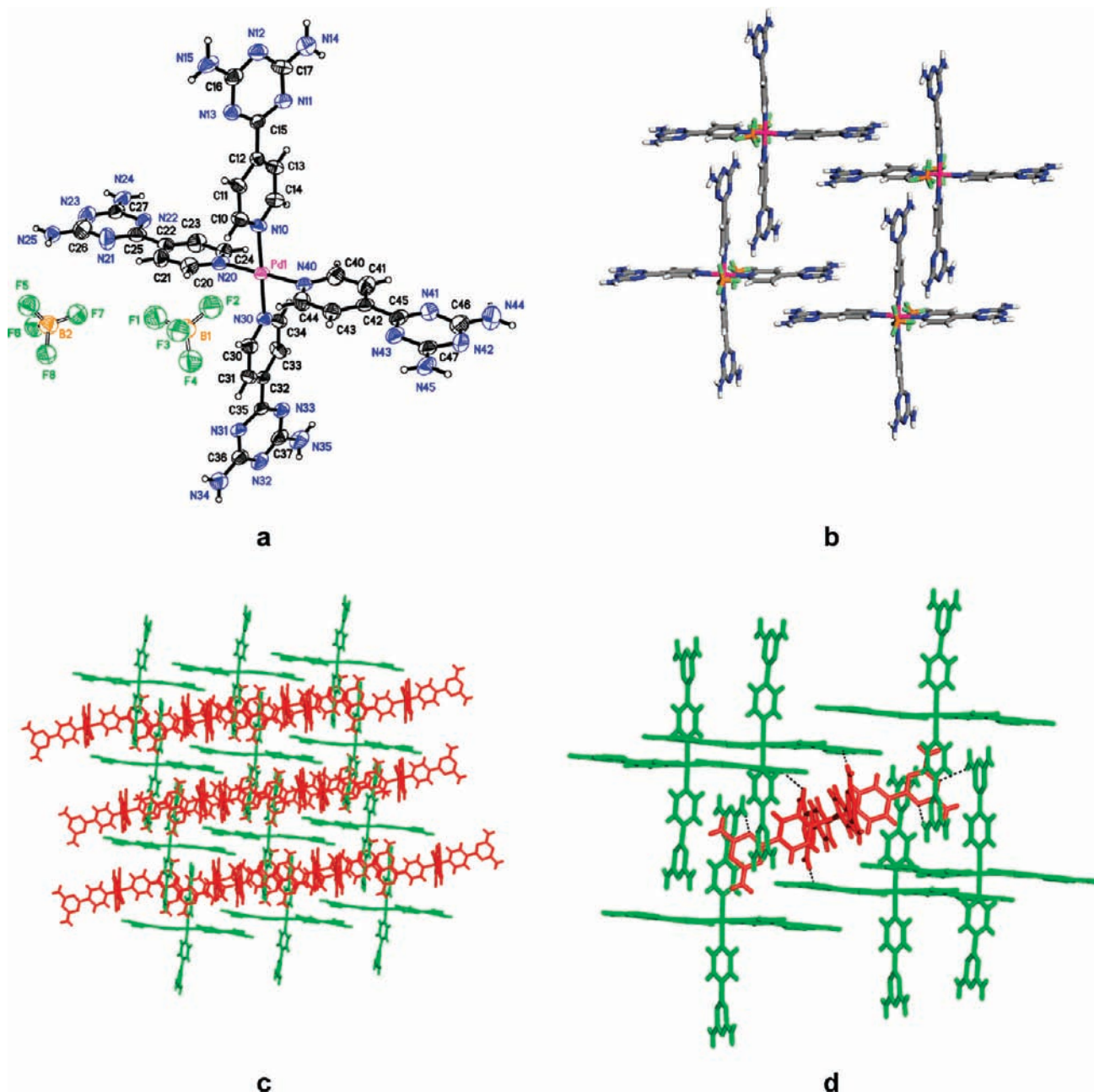
Figure 6. Structure of complex $[Pd(3a)_4](BF_4)_2 \cdot 9H_2O$ in crystals grown from DMSO/H$_2$O/MeCN. Except where noted otherwise, carbon atoms are shown in gray, hydrogen atoms in white, boron atoms in orange, nitrogen atoms in blue, fluorine atoms in green, and palladium atoms in rose. (a) Thermal atomic displacement ellipsoid plot, with ellipsoids of non-hydrogen atoms drawn at the 50% probability level and hydrogen atoms represented by a sphere of arbitrary size. Key bond lengths include Pd1−N10 = 2.031(3) Å, Pd1−N20 = 2.024(4) Å, Pd1−N30 = 2.027(3) Å, and Pd1−N40 = 2.029(3) Å. Representative bond angles include N10−Pd1−N20 = 89.42(13)°. (b) View showing the construction of cationic grids built from tetrameric aggregates. Guest molecules of H$_2$O and BF$_4^-$ are omitted for clarity. (c) View illustrating the interpenetration of grids, with one drawn in green and three independent grids in red. (d) View showing N−H···N hydrogen bonds between molecules in the green and red grids.

hydrogen bonding between DAT groups is reinforced by bridging nitrate anions.

As planned, both ligand **3a** and extended version **3b** form square-planar dicationic Pd(II) complexes analogous to structure **7**. The resulting metallotectons have similar topologies and a shared ability to engage in hydrogen bonding directed by peripheral DAT groups, yet their patterns of association are distinctly different. The observed differences may arise in part because the counterions are not the same and because the crystallizations are

necessarily conducted in solvents that can compete with DAT groups as participants in hydrogen bonding.

*c. Structure of the 4:1 Complex of 6-(Pyridin-3-yl)-1,3, 5-triazine-2,4-diamine (**4a**) with Pd(PF$_6$)$_2$.* The solid formed by the reaction of Pd(BF$_4$)$_2$ with isomeric ligand **4a** proved to have low solubility, so it was subjected to metathesis by the addition of excess NaPF$_6$ in H$_2$O/MeCN, and crystals of the ion-exchanged product were grown from DMSO/H$_2$O/EtOH. They were found to have the composition $[Pd(4a)_4](PF_6)(OH) \cdot 4H_2O \cdot 2EtOH$ and to

Table 2. Crystallographic Data for 1:4 Complexes of Pd(II) with Pyridinyl-Substituted Diaminotriazines 3a,b and 4a,b

complex	$[Pd(3a)_4](BF_4)_2 \cdot 9H_2O$	$[Pd(3b)_4](NO_3)_2 \cdot$ $5DMSO \cdot 2H_2O \cdot MeOH$	$[Pd(4a)_4](PF_6)(OH) \cdot$ $4H_2O \cdot 2EtOH$	$[Pd(4b)_4](NO_3)_2 \cdot$ $6DMSO \cdot 4H_2O$
crystallization medium	DMSO/H$_2$O/MeCN	DMSO/H$_2$O/MeOH	DMSO/H$_2$O/EtOH	DMSO/H$_2$O
formula	$C_{32}H_{50}B_2F_8N_{24}O_9Pd$	$C_{67}H_{86}N_{26}O_{14}PdS_5$	$C_{36}H_{53}F_6N_{24}O_7PPd$	$C_{68}H_{92}N_{26}O_{16}PdS_6$
cryst syst	monoclinic	triclinic	monoclinic	monoclinic
space group	$P2_1/n$	$P\bar{1}$	$C2/m$	$C2/m$
a (Å)	15.2752(3)	11.4019(17)	12.914(3)	20.6228(6)
b (Å)	18.5707(4)	16.516(2)	20.449(3)	21.2334(6)
c (Å)	17.5545(4)	24.136(3)	11.744(4)	15.2728(5)
α (deg)	90	95.452(7)	90	90
β (deg)	98.680(1)	91.174(6)	101.709(6)	126.999(1)
γ (deg)	90	108.713(6)	90	90
V (Å^3)	4922.67(18)	4279.2(11)	3036.9(12)	5341.2(3)
Z	4	2	2	2
ρ_{calc} (g cm^{-3})	1.612	1.355	1.296	1.132
T (K)	200	150	150	150
μ (mm^{-1})	3.987	3.500	3.400	3.016
R_1, $I > 2\sigma(I)$	0.0769	0.0709	0.0528	0.0620
R_1, all data	0.0791	0.0901	0.0529	0.0623
wR_2, $I > 2\sigma(I)$	0.1869	0.1536	0.1736	0.1579
wR_2, all data	0.1884	0.1560	0.1739	0.1585
measured reflns	67694	60316	24003	41486
independent reflns	8948	15194	2709	4841
observed reflns $[I > 2\sigma(I)]$	7082	6471	2703	4337

belong to the monoclinic space group $C2/m$. Views of the structure are shown in Figure 8, and other crystallographic data are presented in Table 2. As expected, a square-planar complex is formed (Figure 8a), with a normal Pd—N distances.[14] The ligands adopt flattened conformations, and their average planes lie at an average angle of 63.9(1)° with respect to the PdN$_4$ core of the metallotecton. The DAT groups of trans-disposed ligands have an opposed orientation, with one DAT group above the PdN$_4$ plane and the other below it.

The structure can be considered to consist of cationic sheets in the ab plane, in which the four DAT groups of each metallotecton participate in a total of 16 N—H···N hydrogen bonds (Figure 8b). Each DAT group engages in two N—H···N hydrogen bonds of type **III**, as well as two additional single N—H···N hydrogen bonds. The extensively hydrogen-bonded structure is also reinforced by aromatic interactions. The cationic sheets are separated by intervening anionic layers containing hydrogen-bonded PF$_6^-$, disordered OH$^-$, H$_2$O, and EtOH (Figure 8c). Again, the complexation of ligand **4a** with Pd(II) occurs predictably to give a square planar metallotecton analogous to structure **7**, and the peripheral DAT groups play a key role in directing molecular association by engaging in hydrogen bonds according to established patterns.

*d. Structure of the 4:1 Complex of 6-[4-(Pyridin-3-yl)phenyl]-1,3,5-triazine-2,4-diamine (**4b**) with Pd(NO$_3$)$_2$.* To complete our assessment of the ability of pyridinyl-substituted diaminotriazines to form metallotectons related to complex **7**, we examined the product of the reaction of extended ligand **4b** with Pd(NO$_3$)$_2$. Crystals grown from DMSO/H$_2$O proved to have the approximate composition $[Pd(4b)_4](NO_3)_2 \cdot 6DMSO \cdot 4H_2O$ and to belong to the monoclinic space group $C2/m$. Figure 9 provides views of the structure, and Table 2 summarizes other

crystallographic data. As planned, coordination yields a square-planar complex (Figure 9a), with a normal Pd—N distances.[14] The ligands adopt flattened conformations, and their average planes form an average angle of 76.3(1)° with respect to the PdN$_4$ core of the metallotecton. The DAT groups of trans-disposed ligands have an opposed orientation, with one DAT group above the PdN$_4$ plane and the other below it, giving the metallotecton an elongated topology. As shown in Figure 9b, the metallotectons associate to form sheets maintained by N—H···N hydrogen bonds of type **I**. Other interactions help control the overall molecular organization, including N—H···O hydrogen bonds involving two types of bridging DMSO, one that reinforces motif **I** (average N—H···O distance = 2.888(6) Å) and the other that helps orient adjacent arms of each metallotecton (N—H···O distance = 3.038(3) Å).

■ CONCLUSIONS

Our results provide a deeper understanding of how coordinative bonds to metals can be used in conjunction with other interactions to direct molecular assembly. In particular, our work illustrates how materials with predictable structural features can be built from metallotectons, which are well-defined complexes incorporating ligands that can bind metals and can simultaneously engage in multiple intercomplex interactions according to reliable motifs. To further gauge the potential of this approach, we have examined the behavior of Pd(II) complexes of ligands **3a,b**, **4a,b**, and **6**, which incorporate pyridinyl groups to bind metals and DAT groups to help ensure participation in reliable intermolecular hydrogen bonds.

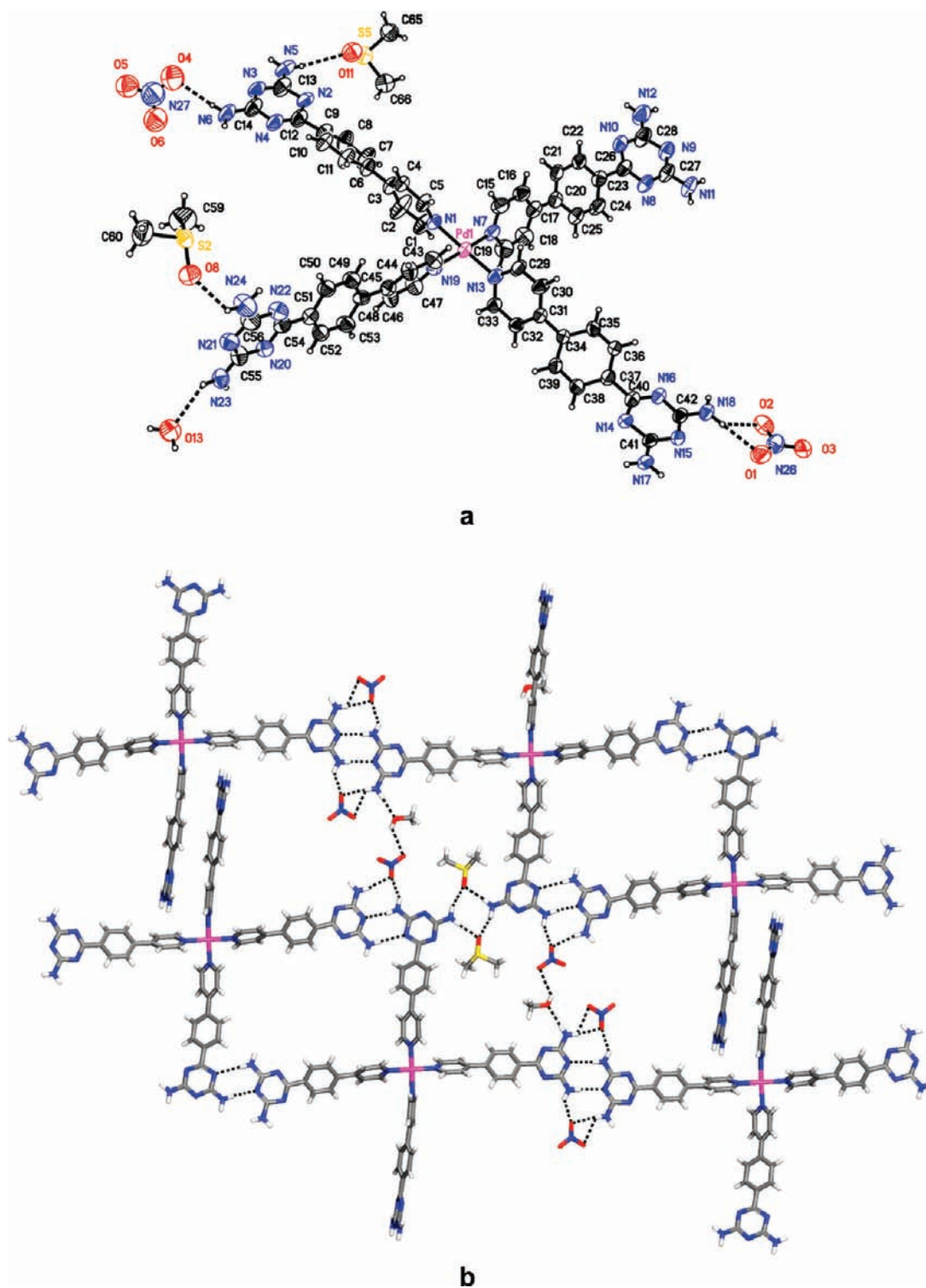As planned, on the basis of established patterns of coordination involving pyridine and simple derivatives, ligands **3a,b**, **4a,b**,

Figure 7. Structure of complex $[Pd(3b)_4](NO_3)_2 \cdot 5DMSO \cdot 2H_2O \cdot MeOH$ in crystals grown from $DMSO/H_2O/MeOH$. Hydrogen bonds are represented by broken lines. Carbon atoms are shown in gray, hydrogen atoms in white, nitrogen atoms in blue, oxygen atoms in red, sulfur atoms in yellow, and palladium atoms in rose. (a) Thermal atomic displacement ellipsoid plot, with ellipsoids of non-hydrogen atoms drawn at the 50% probability level and hydrogen atoms represented by a sphere of arbitrary size. Key bond lengths include $Pd1-N1 = 2.032(5)$ Å, $Pd1-N7 = 1.983(5)$ Å, $Pd1-N13 = 1.997(5)$ Å, and $Pd1-N19 = 2.023(5)$ Å. Representative bond angles include $N1-Pd1-N7 = 90.07(19)°$. (b) View showing how $N-H\cdots N$ hydrogen bonds of type **II** (average distance = 3.084(9) Å) join the metallotectons to form dimers, which interact with adjacent dimers by additional $N-H\cdots N$ hydrogen bonds of type **I** (3.054(7) Å), $N-H\cdots O$ hydrogen bonds involving bridging molecules of DMSO (average distance = 2.936(8) Å), and aromatic interactions.

and **6** all bind Pd(II) to gave square-planar complexes with predicted constitutions. Although the precise geometry of the

resulting metallotectons could not be foreseen with confidence, in all cases, the ligands adopted normal flattened conformations
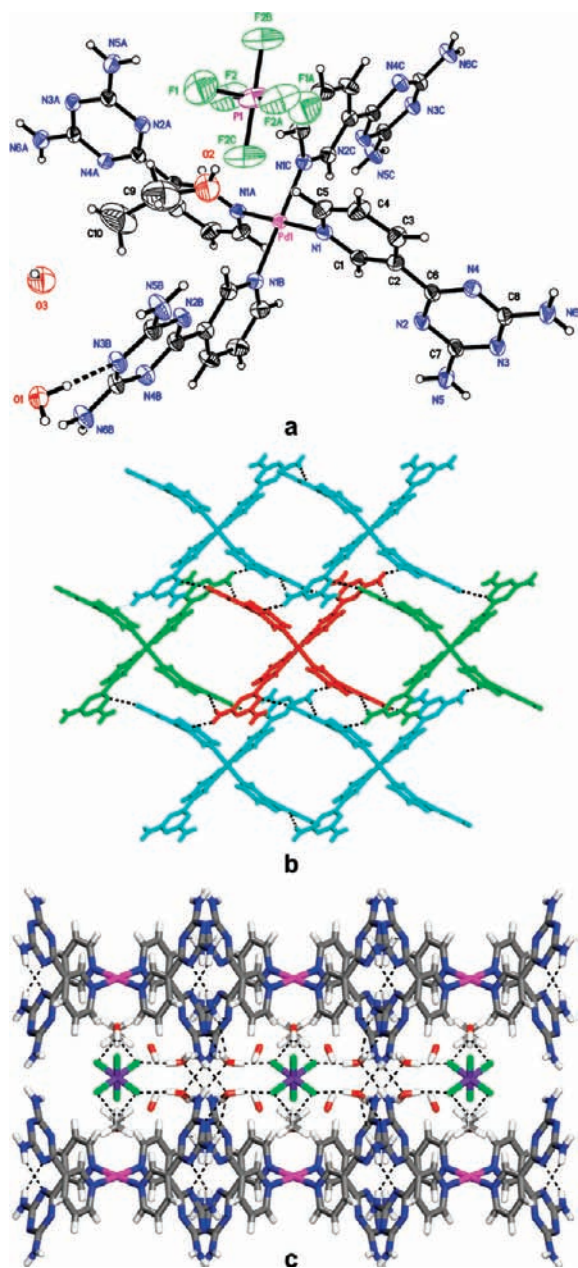
and maintained expected orientations with respect to the PdL$_4$ core. As anticipated, subsequent association of the resulting metallotectons was found to be directed in part by their logical topologies and by the ability of the peripheral DAT groups to engage in intermolecular hydrogen bonding according to established motifs I–III. In only one case were such interactions not present.

Complexes of ligands 3a,b, 4a,b, and 6 have shared structural features that can be considered to be introduced reliably by design. However, comparisons of molecular organization reveal few striking analogies, and structural details vary widely, particularly in the ionic PdL$_4$$^{2+}$ complexes. These differences presumably reflect diverse factors, such as the contributions of ionic interactions, the role of the specific anions, and competitive hydrogen bonding involving molecules of solvent.

Despite the present lack of perfect control, our work nevertheless affirms the promise of designing new ordered materials based on the hybrid inorganic/organic strategy of using metallotectons. A conspicuous advantage of this strategy is that the molecular core can be constructed spontaneously by coordination, and peripheral functionality can independently control how the complexes are positioned with respect to their neighbors.

■ EXPERIMENTAL SECTION

General Notes. 6-(Pyridin-4-yl)-1,3,5-triazine-2,4-diamine (3a),[8] 6-[4-(pyridin-4-yl)phenyl]-1,3,5-triazine-2,4-diamine (3b),[9] 6-(pyridin-3-yl)-1,3,5-triazine-2,4-diamine (4a),[10] 6-[4-(pyridin-3-yl)phenyl]-1,3,5-triazine-2,4-diamine (4b),[11] and 6-(pyridin-2-yl)-1,3,5-triazine-2,4-diamine (6)[15] were prepared by reported methods. Their complexes with Pd(II) were made by the procedures summarized below. Other chemicals were purchased from commercial sources and used without further purification.

General Procedure for Preparing PdCl$_2$ Complexes of Ligands 3a,b, 4a,b, and 6. A stirred suspension of PdCl$_2$ (1.0 equiv) and the ligand (2.0 equiv in the cases of compounds 3a,b and 4a, b; 1.0 equiv in the case of compound 6) was heated at reflux in MeCN (20 mL) for 12 h. The resulting mixture was cooled, and precipitated solids were separated by filtration. The solids were washed thoroughly with H$_2$O, MeCN, and acetone. The product was then finally dried under vacuum before being purified by crystallization.

2:1 Complex of 6-(Pyridin-4-yl)-1,3,5-triazine-2,4-diamine (3a) with PdCl$_2$ (Orthorhombic Form). The reaction of ligand 3a (51 mg, 0.27 mmol) with PdCl$_2$ (24 mg, 0.14 mmol) according to the general procedure yielded the crude 2:1 complex (62 mg, 0.11 mmol, 81%). Pale yellow crystals of composition PdCl$_2$(3a)$_2$·2DMSO were grown by allowing H$_2$O to diffuse slowly into a solution in DMSO. IR (ATR): 3429, 3330, 3202, 1651, 1614, 1529, 1445, 1421, 1398, 1061, 811 cm^{-1}. HRMS (ESI) calcd for [C$_{16}$H$_{16}$ClN$_{12}$Pd]$^+$: m/e 517.03388. Found: 517.03406.

2:1 Complex of 6-(Pyridin-4-yl)-1,3,5-triazine-2,4-diamine (3a) with PdCl$_2$ (Triclinic Form). The crude 2:1 complex was prepared as described above, and pale yellow crystals of composition PdCl$_2$(3a)$_2$·2DMSO· dioxane were grown by slow evaporation of a solution in DMSO/dioxane. IR (ATR): 3429, 3330, 3202, 1651, 1614, 1529, 1445, 1421, 1398, 1061, 811 cm^{-1}. HRMS (ESI) calcd for [C$_{16}$H$_{16}$ClN$_{12}$Pd]$^+$: m/e 517.03388. Found: 517.03406.

2:1 Complex of 6-[4-(Pyridin-4-yl)phenyl]-1,3,5-triazine-2,4-diamine (3b) with PdCl$_2$. The reaction of ligand 3b (80 mg, 0.30 mmol) with PdCl$_2$ (27 mg, 0.15 mmol) according to the general procedure yielded the crude 2:1 complex (88 mg, 0.12 mmol, 80%). Pale yellow crystals of composition PdCl$_2$(3b)$_2$ were grown by slow evaporation of a solution in DMSO/EtOAc. IR (ATR): 3481, 3435, 3395, 3303, 3129, 1613, 1586, 1520, 1436, 1396, 808 cm^{-1}. HRMS (ESI) calcd for
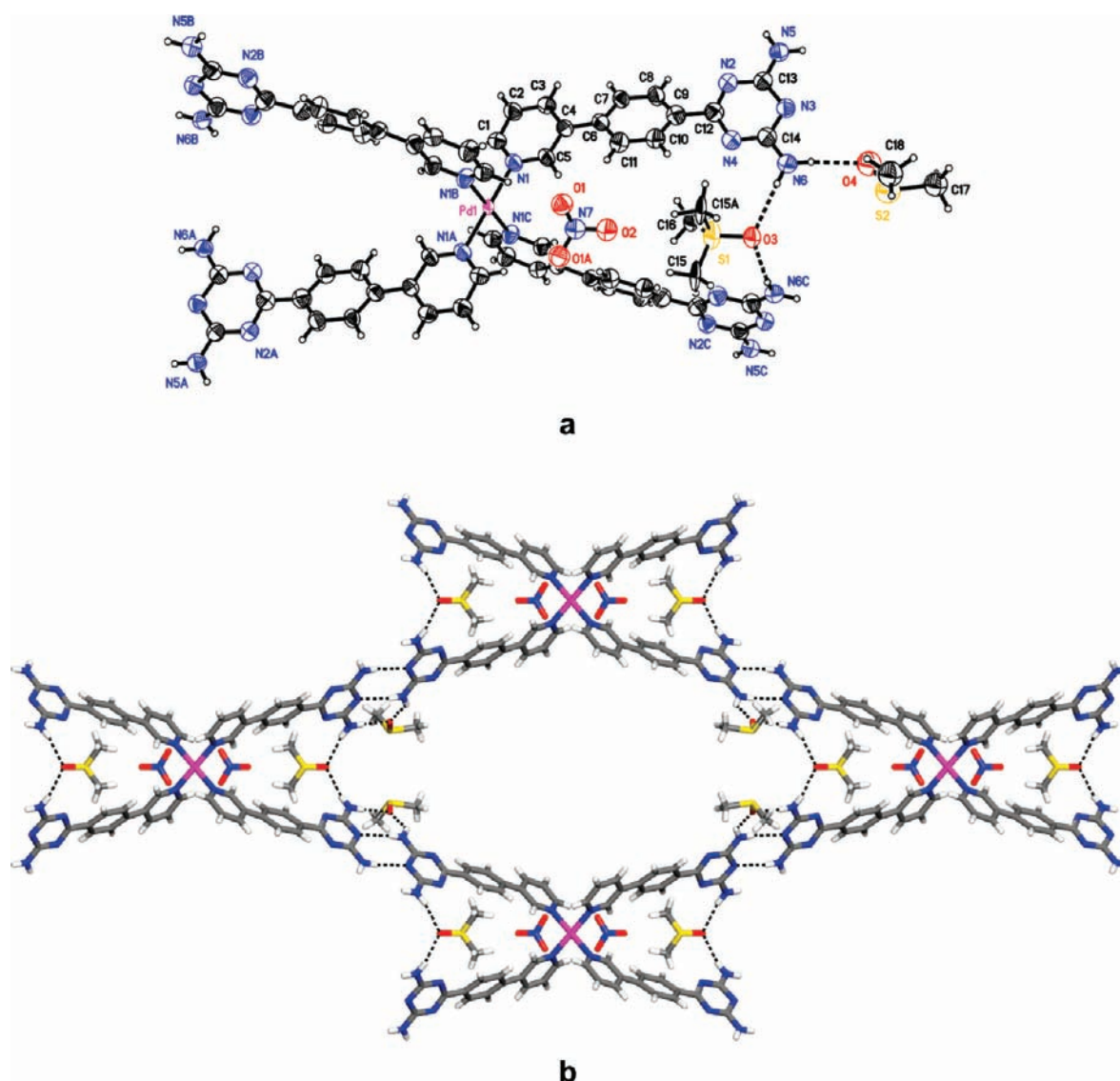

Figure 8. Structure of complex [Pd(4a)$_4$](PF$_6$)(OH)·4H$_2$O·2EtOH in crystals grown from DMSO/H$_2$O/EtOH. Except where noted otherwise, carbon atoms are shown in gray, hydrogen atoms in white, nitrogen atoms in blue, fluorine atoms in green, phosphorus atoms in purple, and palladium atoms in rose. (a) Thermal atomic displacement ellipsoid plot, with ellipsoids of non-hydrogen atoms drawn at the 50% probability level and hydrogen atoms represented by a sphere of arbitrary size. Key bond lengths include Pd1–N1 = 2.023(4) Å. Representative bond angles include N1–Pd1–N1B = 90.95(19)°. (b) View showing the formation of cationic sheets in the *ab* plane, in which the four DAT groups of a central metallotecton (red) engage in a total of 16 N–H···N hydrogen bonds with six neighbors (blue and green). Each DAT group forms two N–H···N hydrogen bonds of type III (3.091(6) Å) involving the two neighbors shown in green, as well as two additional single N–H···N hydrogen bonds (3.069(6) Å) with neighbors in red. In addition, the structure is reinforced by aromatic interactions. Neutral guests and counterions are omitted for clarity. (c) View along the *a* axis showing how cationic sheets of the metallotecton are separated by intervening anionic layers containing hydrogen-bonded PF$_6$$^-$, disordered OH$^-$, H$_2$O, and EtOH.

Figure 9. Structure of complex $[Pd(4b)_4](NO_3)_2 \cdot 6DMSO \cdot 4H_2O$ in crystals grown from DMSO/H$_2$O. Hydrogen bonds are represented by broken lines. Carbon atoms are shown in gray, hydrogen atoms in white, nitrogen atoms in blue, oxygen atoms in red, sulfur atoms in yellow, and palladium atoms in rose. (a) Thermal atomic displacement ellipsoid plot, with ellipsoids of non-hydrogen atoms drawn at the 50% probability level and hydrogen atoms represented by a sphere of arbitrary size. Key bond lengths include Pd1–N1 = 2.046(2) Å. Representative bond angles include N1–Pd1–N1B = 90.81(11)°. (b) View showing the formation of sheets held together by N–H···N hydrogen bonds of type **I** (2.955(5) Å), reinforced by N–H···O hydrogen bonds involving bridging molecules of DMSO.

$[C_{28}H_{24}ClN_{12}Pd]^+$: m/e 669.09648. Found: 669.09845. Anal. Calcd for $C_{28}H_{24}Cl_2N_{12}Pd$: C, 47.64; H, 3.43; N, 23.81. Found: C, 47.49; H, 3.27; N, 23.32.

*2:1 Complex of 6-(Pyridin-3-yl)-1,3,5-triazine-2,4-diamine (**4a**) with PdCl$_2$.* The reaction of ligand **4a** (74 mg, 0.39 mmol) with PdCl$_2$ (35 mg, 0.20 mmol) according to the general procedure yielded the crude 2:1 complex (79 mg, 0.14 mmol, 72%). Pale yellow crystals of composition PdCl$_2$(**4a**)$_2$·3DMSO were grown by slow evaporation of a solution in DMSO. IR (ATR): 3465, 3382, 3323, 3196, 3140, 1626, 1614, 1546, 1397, 805 cm^{-1}. HRMS (ESI) calcd for $[C_{16}H_{16}ClN_{12}Pd]^+$ m/e: 517.03388. Found: 517.03405. Anal. Calcd for $C_{16}H_{16}Cl_2N_{12}Pd \cdot H_2O$: C, 33.61; H, 3.17; N, 29.40. Found: C, 33.37; H, 3.06; N, 28.68.

*1:1 Complex of 6-(Pyridin-2-yl)-1,3,5-triazine-2,4-diamine (**6**) with PdCl$_2$.* The reaction of ligand **6** (67 mg, 0.36 mmol) with PdCl$_2$ (63 mg, 0.36 mmol) according to the general procedure yielded the crude 1:1 complex (116 mg, 0.32 mmol, 89%). Yellow crystals of composition

PdCl$_2$(**6**) were grown by slow evaporation of a solution in DMSO/H$_2$O. IR (ATR): 3448, 3400, 3188, 3119, 1659, 1634, 1581, 1518, 1489, 1397, 1262, 1058, 1031, 779 cm^{-1}. HRMS (ESI) calcd for $[C_8H_8ClN_6Pd]^+$: m/e 328.95283. Found: 328.95347. Anal. Calcd for $C_8H_8Cl_2N_6Pd$: C, 26.29; H, 2.21; N, 22.91. Found: C, 26.28; H, 2.26; N, 22.35.

General Procedures for Preparing Other Pd(II) Complexes of Ligands 3a,b and 4a,b. A stirred suspension of Pd(BF$_4$)$_2$ or Pd(NO$_3$)$_2$ (1.0 equiv) and the ligand (4.0 equiv) was heated at reflux in MeCN (20 mL) for 12 h. The resulting mixture was cooled, and precipitated solids were separated by filtration. The solids were washed thoroughly with H$_2$O, MeCN, and acetone. The product was then finally dried under vacuum before being purified by crystallization. In the case of the complex of ligand **4a** with Pd(BF$_4$)$_2$, the crude product was subjected to ion exchange before crystallization by treatment with excess NaPF$_6$ in H$_2$O/MeCN.

*4:1 Complex of 6-(Pyridin-4-yl)-1,3,5-triazine-2,4-diamine (**3a**) with Pd(BF$_4$)$_2$.* The reaction of ligand **3a** (80 mg, 0.43 mmol) with

Pd(BF$_4$)$_2$·4MeCN (47 mg, 0.11 mmol) according to the general procedure yielded the crude 4:1 complex (87 mg, 0.084 mmol, 78%). Colorless crystals of composition [Pd(**3a**)$_4$](BF$_4$)$_2$·9H$_2$O were grown by allowing H$_2$O and MeCN to diffuse slowly into a solution in DMSO. IR (ATR): 3500–3000 (b), 1615, 1425, 1392, 1301, 1217, 957, 821 cm^{-1}. HRMS (ESI) calcd for [C$_{32}$H$_{32}$N$_{24}$Pd]$^{2+}$: *m/e* 429.11383. Found: 429.11505. Anal. Calcd for C$_{32}$H$_{32}$B$_2$F$_8$N$_{24}$Pd·2H$_2$O: C, 35.96; H, 3.40; N, 31.45. Found: C, 35.91; H, 3.10; N, 30.86.

*4:1 Complex of 6-[4-(Pyridin-4-yl)phenyl]-1,3,5-triazine-2,4-diamine (**3b**) with Pd(NO$_3$)$_2$.* The reaction of ligand **3b** (55 mg, 0.21 mmol) with Pd(NO$_3$)$_2$ (12 mg, 0.052 mmol) according to the general procedure yielded the crude 4:1 complex (57 mg, 0.044 mmol, 85%). Yellow crystals of composition [Pd(**3b**)$_4$](NO$_3$)$_2$·5DMSO·2H$_2$O·MeOH were grown by allowing H$_2$O and MeOH to diffuse slowly into a solution in DMSO. IR (ATR): 3319, 3100 (b), 1612, 1526, 1438, 1394, 1324, 811 cm^{-1}. HRMS (ESI) calcd for [C$_{56}$H$_{48}$N$_{24}$Pd]$^{2+}$: *m/e* 581.17588. Found: 581.17864. Anal. Calcd for C$_{56}$H$_{48}$N$_{26}$O$_6$Pd: C, 52.24; H, 3.76; N, 28.28. Found: C, 52.30; H, 3.71; N, 27.74.

*4:1 Complex of 6-(Pyridin-3-yl)-1,3,5-triazine-2,4-diamine (**4a**) with Pd(PF$_6$)$_2$.* The reaction of ligand **4a** (76 mg, 0.40 mmol) with Pd(BF$_4$)$_2$ (28 mg, 0.10 mmol) according to the general procedure yielded a solid, which was then treated with NaPF$_6$ (67 mg, 0.40 mmol) in a mixture of H$_2$O (10 mL) and MeCN (10 mL) to give the crude 4:1 complex (82 mg, 0.071 mmol, 71%). Colorless crystals of composition [Pd(**4a**)$_4$]-(PF$_6$)(OH)·4H$_2$O·2EtOH were grown by allowing H$_2$O and EtOH to diffuse slowly into a solution in DMSO. IR (ATR): 3469, 3349, 3100 (b), 1625, 1536, 1450, 1382, 1023, 807 cm^{-1}. HRMS (ESI) calcd for [C$_{32}$H$_{32}$N$_{24}$Pd]$^{2+}$: *m/e* 429.11383. Found: 429.11355.

*4:1 Complex of 6-[4-(Pyridin-3-yl)phenyl]-1,3,5-triazine-2,4-diamine (**4b**) with Pd(NO$_3$)$_2$.* The reaction of ligand **4b** (60 mg, 0.23 mmol) with Pd(NO$_3$)$_2$ (14 mg, 0.061 mmol) according to the general procedure yielded the crude 4:1 complex (65 mg, 0.050 mmol, 87%). Yellow crystals of composition [Pd(**4b**)$_4$](NO$_3$)$_2$·6DMSO·4H$_2$O were grown by allowing H$_2$O to diffuse slowly into a solution in DMSO. IR (ATR): 3475, 3307, 3166, 1623, 1527, 1447, 1390, 789 cm^{-1}. HRMS (ESI) calcd for [C$_{56}$H$_{48}$N$_{24}$Pd]$^{2+}$: *m/e* 581.17588. Found: 581.17864. Anal. Calcd for C$_{56}$H$_{48}$N$_{26}$O$_6$Pd: C, 52.24; H, 3.76; N, 28.28. Found: C, 52.21; H, 3.72; N, 27.35.

X-Ray Crystallographic Studies. Crystallographic data were collected with Cu Kα radiation at the temperatures indicated in Tables 1 and 2 using a Bruker Microstar diffractometer equipped with a rotating anode. Intensity data were integrated using the *SAINT* program,[16] and semiempirical absorption corrections were applied using the *SADABS* program.[17] The structures were solved by direct methods, and non-hydrogen atoms were refined anisotropically on F^2 with full least squares using the *SHELXL-97* software package.[18] In most cases, hydrogen atoms of ligands and guest molecules were treated by first locating them from difference Fourier maps, recalculating their positions using standard values for distances and angles, and then refining them as riding atoms. Hydrogen atoms from water molecules were located directly and refined using restraints.

In complex PdCl$_2$(**3a**)$_2$·2DMSO, the complex and the included molecules of DMSO lie on a 2-fold axis, which results in statistical disorder over two positions with a half-occupancy factor for each atom of chlorine and DMSO. Certain molecules of DMSO are also disordered in crystals of composition PdCl$_2$(**3a**)$_2$·2DMSO·dioxane, PdCl$_2$-(**4a**)$_2$·3DMSO, and [Pd(**3b**)$_4$](NO$_3$)$_2$·5DMSO·2H$_2$O·MeOH. In crystals of composition [Pd(**4b**)$_4$](NO$_3$)$_2$·6DMSO·4H$_2$O, DMSO lies on a mirror plane, giving two alternative positions for one of the methyl groups with a half-occupancy factor. In certain cases, guest molecules proved to be significantly disordered and could not be modeled properly; therefore, the SQUEEZE option in the *PLATON* software package[19] was used to calculate the region of solvent disorder and to remove its contribution from the overall intensity data.

In the case of crystals of composition [Pd(**4a**)$_4$](PF$_6$)(OH)·4H$_2$O·2-EtOH, the structural solution led to the position of the Pd center with one attached ligand **4a**, half a PF$_6^-$ counterion, three atoms from a guest molecule of EtOH, and two isolated atoms of oxygen. After subsequent cycles of least-squares refinement, the positions of two atoms of hydrogen linked to one of the isolated atoms of oxygen were clearly visible in the Fourier difference map, revealing a molecule of H$_2$O that is doubly hydrogen bonded. The second isolated atom of oxygen was found to be disordered over four symmetry-related positions. The closest peak of high electron density found in the difference Fourier map was attributed to an atom of hydrogen, thereby defining an OH$^-$ and assuring charge balance in the crystal lattice.

■ ASSOCIATED CONTENT

Ⓢ **Supporting Information.** Tables of structural data in CIF format. This material is available free of charge via the Internet at http://pubs.acs.org.

■ AUTHOR INFORMATION

Corresponding Author
*E-mail: james.d.wuest@umontreal.ca.

■ ACKNOWLEDGMENT

■ REFERENCES

(1) Bragg, W. L. *Proc. R. Soc. London* **1913**, *89*, 248–277.

(2) Allen, F. H. *Acta Crystallogr.* **2002**, *B58*, 380–388.

(3) Dunitz, J. D.; Gavezzotti, A. *Chem. Soc. Rev.* **2009**, *38*, 2622–2633. Dunitz, J. D. *Chem. Commun.* **2003**, 545–548. Desiraju, G. R. *Nat. Mater.* **2002**, *1*, 77–79. Gavezzotti, A. *Acc. Chem. Res.* **1994**, *27*, 309–314. Maddox, J. *Nature* **1988**, *335*, 201.

(4) For references, see: Ward, M. D. *Struct. Bonding (Berlin)* **2009**, *132*, 1–23. Robson, R. *Dalton Trans.* **2008**, 5113–5131. Wuest, J. D. *Chem. Commun.* **2005**, 5830–5837. Hosseini, M. W. *Acc. Chem. Res.* **2005**, *38*, 313–323. Nangia, A.; Desiraju, G. R. *Top. Curr. Chem.* **1998**, *198*, 57–95. Desiraju, G. R. *Angew. Chem., Int. Ed.* **1995**, *34*, 2311–2327. Etter, M. C. *Acc. Chem. Res.* **1990**, *23*, 120–126.

(5) Telfer, S. G.; Wuest, J. D. *Cryst. Growth Des.* **2009**, *9*, 1923–1931. Wan, C.-Q.; Li, G.-S.; Chen, X.-D.; Mak, T. C. W. *Cryst. Growth Des.* **2008**, *8*, 3897–3901. Constable, E. C.; Housecroft, C. E.; Neuberger, M.; Schaffner, S.; Schaper, F. *Inorg. Chem. Commun.* **2006**, *9*, 433–436.

(6) For reviews, see: Braga, D.; Brammer, L.; Champness, N. R. *CrystEngComm* **2005**, *7*, 1–19. Brammer, L. *Chem. Soc. Rev.* **2004**, *33*, 476–489. Aakeröy, C. B.; Beatty, A. M. In *Comprehensive Coordination Chemistry II*; McCleverty, J. A., Meyer, T. J., Lever, A. B. P., Eds.; Elsevier: Oxford, 2004; Vol. 1, pp 679–688. Beatty, A. M. *Coord. Chem. Rev.* **2003**, *246*, 131–143.

(7) Ouerfelli, I.; Gatri, R.; Efrit, M. L.; Dua, N.; Perruchon, J.; Golhen, S.; Toupet, L.; Fillaut, J.-L. *J. Organomet. Chem.* **2011**, *696*, 670–675. Santillan, G. A.; Carrano, C. J. *Dalton Trans.* **2009**, 6599–6605. McMorran, D. A. *Inorg. Chem.* **2008**, *47*, 592–601. Salazar-Mendoza, D.; Baudron, S. A.; Hosseini, M. W. *Chem. Commun.* **2007**, 2252–2254. Braga, D.; Giaffreda, S. L.; Grepioni, F.; Maini, L.; Polito, M. *Coord. Chem. Rev.* **2006**, *250*, 1267–1285. Goldberg, I. *Chem. Commun.* **2005**, 1243–1254. Katsuki, I.; Motoda, Y.; Sunatsuki, Y.; Matsumoto, N.; Nakashima, T.; Kojima, M. *J. Am. Chem. Soc.* **2002**, *124*, 629–640.

(8) Chan, C.-W.; Mingos, D. M. P.; White, A. J. P.; Williams, D. J. *Polyhedron* **1996**, *15*, 1753–1767.

(9) Duong, A.; Dubois, M.-A.; Maris, T.; Métivaud, V.; Yi, J.-H.; Nanci, A.; Rochefort, A.; Wuest, J. D. *J. Phys. Chem. C* **2011**, *115*, in press.

(10) Baibulova, M. S.; Akkulova, Z. G.; Afanas'eva, T. A. *Izv. Akad. Nauk Kazakh. SSR, Ser. Khim.* **1989**, 40–42.

(11) Duong, A.; Maris, T.; Wuest, J. D. *Cryst. Growth Des.* **2011**, *11*, 287–294.

(12) For recent references, see: Maly, K. E.; Gagnon, E.; Maris, T.; Wuest, J. D. *J. Am. Chem. Soc.* **2007**, *129*, 4306–4322.

(13) Lee, H. M.; Liao, C.-Y. *Acta Crystallogr.* **2008**, *E64*, m1447. Liao, C.-Y.; Lee, H. M. *Acta Crystallogr.* **2006**, *E62*, m680–m681. Viossat, B.; Dung, N.-H.; Robert, F. *Acta Crystallogr.* **1993**, *C49*, 84–85.

(14) De León, A.; Pons, J.; Solans, X.; Font-Bardia, M. *Acta Crystallogr.* **2007**, *E63*, m2164. Ma, L.; Smith, R. C.; Protasiewicz, J. D. *Inorg. Chim. Acta* **2005**, *358*, 3478–3482. Holzbock, J.; Sawodny, W.; Thewalt, U. *Z. Anorg. Allg. Chem.* **2000**, *626*, 2563–2568.

(15) Case, F. H.; Koft, E. *J. Am. Chem. Soc.* **1959**, *81*, 905–906.

(16) *SAINT*, version 7.68A; Bruker AXS Inc.: Madison, WI 53719-1173, 2009.

(17) Sheldrick, G. M. *SADABS*, version 2008/1; Bruker AXS Inc.: Madison, WI 53719-1173, 2008.

(18) Sheldrick, G. M. *Acta Crystallogr.* **2008**, *A64*, 112–122.

(19) Spek, A. L. *PLATON*; Utrecht University: Utrecht, The Netherlands, 2001. van der Sluis, P.; Spek, A. L. *Acta Crystallogr.* **1990**, *A46*, 194–201.

5618

dx.doi.org/10.1021/ic2003047 |*Inorg. Chem.* 2011, 50, 5605–5618